

# PRESSURELESS SINTERING OF $B_4C$ -NANO $TiB_2$ NANOCOMPOSITE BY ADDITION OF Fe AND Ni AS SINTERING AIDS

M. M. Mohammadi Samani<sup>1</sup>, H. R. Baharvandi<sup>1</sup>, H. Abdizadeh<sup>2</sup> and J. Rezapour<sup>1</sup>

\* m3.samani@gmail.com

Received: March 2014

Accepted: September 2014

<sup>1</sup> Malek-Ashtar University of Technology, Tehran, Iran.

<sup>2</sup> School of Metallurgy and Materials Engineering, University of Tehran, Tehran, Iran.

**Abstract:**  $B_4C$  and its composites with  $TiB_2$  as second phase continues to be extensively used as the preferred ceramic material in military applications as armor systems for absorbing and dissipating kinetic energy from high velocity projectiles. It also exhibits a high melting point (2427 °C), and high neutron absorption cross section. Pressureless sintering of the  $B_4C$ -nano $TiB_2$  nanocomposite using small amount of Fe and Ni ( $\leq 3$  Wt%) as sintering aids was investigated in order to clarify the role of Fe and Ni additions on the mechanical and microstructural properties of  $B_4C$ -nano $TiB_2$  nanocomposites. Different amount of Fe and Ni, mainly 1 to 3 Wt% were added to the base material. Pressureless sintering was conducted at 2175, 2225 and 2300 °C. It was found that Addition of 3 Wt% Fe and 3 wt% Ni and sintering at 2300 °C resulted in improving the density of the samples to about 99% of theoretical density. The nanocomposite samples exhibited high density, hardness, and microstructural uniformity.

**Keywords:**  $B_4C$ ;  $TiB_2$ ; Pressureless Sintering; Nanocomposite; Sintering Aid.

## 1. INTRODUCTION

Boron carbide is a low density (2.52 g/cm<sup>3</sup>) ceramic and the third known hardest material (2900–3900 kg/mm<sup>2</sup>), ranking after diamond (8000–8500 kg/mm<sup>2</sup>) and cubic boron nitride (4500–4600 kg/mm<sup>2</sup>).<sup>1</sup> It is the premier material for personal armor typically in the form of front and back inserts into flak jackets in which  $B_4C$  plates are bonded to a polymer backing. It is used in particulate form as an abrasive, and as a nozzle material for slurry pumping and grit blasting because of its excellent abrasion resistance.<sup>[2,6]</sup>

The use of monolithic boron carbide is limited by its low strength, low toughness, poor sinterability and machinability. Since  $B_4C$  is very difficult to be sintered higher than approximately 80% of the theoretical density, a variety of second phases have been added as sintering aids. Significant improvement in sinterability was observed when a small amount of carbon was added before hot pressing.<sup>[3]</sup>

Pressureless sintering of  $B_4C$  to high density, however, has proven difficult. Achieving near-theoretical density has required gang-hot pressing (stacked parts under pressure) which precludes the formation of complex shapes. Additives such as SiC,  $Al_2O_3$ ,  $TiB_2$ ,  $AlF_3$  and

$W_2B_5$  have been used as sintering aids to increase pressureless sintered density, but the second formed phases often have deleterious effects on mechanical behavior. Other additives such as Al, Fe, Ti, B and SiC have also been used, with various degrees of improvement in sintering behavior and mechanical properties.<sup>[2,9]</sup>

However the addition of metallic phases with low melting temperatures generally reduces the physical and mechanical properties of hard ceramics. Also the improvement in sintering behavior of  $B_4C$  by addition of non-oxide ceramics was rather restricted.<sup>4</sup> Among the studied systems,  $B_4C$ -nano $TiB_2$  nanocomposites are promising to be suitable candidates for applications and attracted the attention of materials scientists because of the very interesting mechanical properties associated to micro-cracking behavior that accounts of appealing for high mechanical and microstructural properties.<sup>[5,10]</sup>

The effect of the Fe and Ni addition on the densities is even more pronounced at lower processing temperatures and is related to the presence of a liquid phase in the Fe and Ni-containing material. Limited study has been carried out on addition of nano $TiB_2$  and one of the metallic elements simultaneously as sintering



aids. In the present study, the effect of nanoTiB<sub>2</sub> and Fe or Ni addition as a sintering aid on the densification behavior of B<sub>4</sub>C has been investigated. The resulting microstructure and mechanical properties of the nanocomposite are presented and discussed.

## 2. EXPERIMENTAL PROCEDURE

The main starting material used in the present study consisted of high-purity B<sub>4</sub>C (Chengdu Rong feng china), Titanium (IV) Isopropoxide solution (Alfa Aesar) as Ti supplier, Fe powder (particle size less than 10 μm, Alfa Aesar) and Ni powder (particle size less than 10 μm, Alfa Aesar). The chemical composition of B<sub>4</sub>C powder is given in table 1. NanoTiB<sub>2</sub> powder has been prepared by H. Sinaei Pour Fard experimental route.<sup>7</sup> The average size and the specific surface area of B<sub>4</sub>C powder was measured to be 1.33 μm and 6.64 m<sup>2</sup>/g, respectively.<sup>[4]</sup> Nanocomposites were prepared using constant amounts of nanoTiB<sub>2</sub> (10 Wt%) as secondary phase, Fe (from 0 to 3wt%) and Ni (0 to 3 wt%) as sintering aids. In some of the

samples, powders were mixed with high-purity phenolic resin not only as carbon supplier ( up to 2wt%) but also as binder. Chemical composition of nanocomposites are given in table 2. The mixed powders of each composition were ball milled in Isopropanol with C<sub>3</sub>H<sub>2</sub>OH chemical composition and 99.6% purity as media in planetary ball mill for 2 hr using WC balls. The mixture was then dried in a rotary vacuum evaporator, and passed through a 60 mesh screen. The powder mixtures were cold pressed under 80 MPa into segments (Φ=10 mm, h=10 mm). The green samples were then sintered using controlled graphite element tube furnace under Ar atmosphere at 2175, 2225 and 2300 °C (heating rate = 10 °C/min). After holding for 1 hr at the temperatures, the furnace was shut down and let it cool to room temperature naturally.

Sintered bodies were surface ground and polished with diamond paste down to 1 μm grain size for successive microstructure examinations. The polished surfaces were chemically etched in 30% HF acid solution for 60–120 s. The microstructure was observed under scanning electron microscope (SEM) (JEOL, JSM-5500). Relative density of samples was measured by Archimede’s method (ASTM B311). Crystalline phases were characterized by X-ray diffraction (XRD) (Philips, model XRG3100-PW3710). Data were collected with Ni filtered Cu Kα radiation, in the angular range from 4° to 90° (2Theta degrees). To measure the hardness, a Vickers indenter was used with a load of 1.96 N.

**Table 1.** Chemical composition of B<sub>4</sub>C powder.

Element or compounds	B	C	B <sub>2</sub> O <sub>3</sub>	Fe	Si
wt%	76.1	20.3	1.96	0.73	0.91

**Table 2.** Chemical composition of nanocomposites.

Samples code	F-Series								N-Series						
	F1	F2	F3	F4	F5	F6	F7	F8	N1	N2	N3	N4	N5	N6	N7
B <sub>4</sub> C (wt%)	88	87.5	87	86.5	86	85	88	89	87.5	87	86.5	86	85	88	89
TiB <sub>2</sub> (wt%)	10	10	10	10	10	10	10	10	10	10	10	10	10	10	10
Fe (wt%)	0	0.5	1	1.5	2	3	1	1	0	0	0	0	0	0	0
Ni (wt%)	0	0	0	0	0	0	0	0	0.5	1	1.5	2	3	1	1
C (wt%)	2	2	2	2	2	2	1	0	2	2	2	2	2	1	0

### 3. Results and Discussion

#### 3. 1. X-ray diffraction phase analysis

Figure 1 shows the X-ray diffraction analysis of F6 code from F-Series samples before and after sintering at 2300 °C for 1 hr. According to XRD analysis (Fig. 1-a), the green sample of F6 code just contains B<sub>4</sub>C and TiB<sub>2</sub> phases. After the heat treatment of the green sample, the diffraction peaks associated with four phases, namely B<sub>4</sub>C, TiB<sub>2</sub>, FeB and C (Fig. 1-b). From the ternary Fe-B-C phase diagram at 1273K calculated using “Thermocalc” software (Figure 2), it is clear that Fe corresponds to point A and is located within the three phase (FeB-B<sub>4</sub>C-graphite) region.<sup>8</sup> Thus, interaction between boron carbide and Fe results in the formation of FeB and C (Graphite) releasing according to reaction 1:8

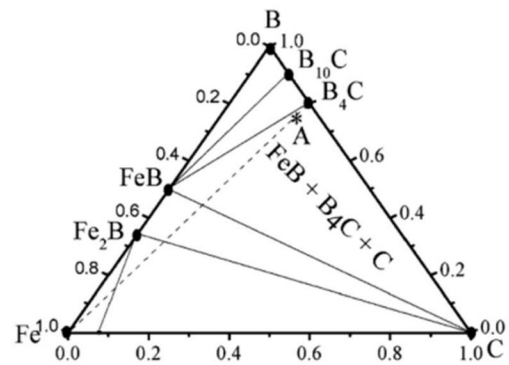
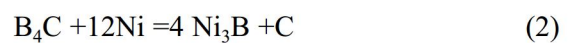


Fig. 2. Isothermal section of the ternary Fe-B-C diagram at 1273 K.



The motivation for using iron powder as an appropriate addition is based on the reaction between Fe and B<sub>4</sub>C that leads to the release of carbon (Graphite) and to the formation of the FeB phase. The relatively low melting point of FeB (1400-1500 °C) provides the conditions for liquid phase sintering of boron carbide. In B<sub>4</sub>C-nanoTiB<sub>2</sub>-Fe system, there is not any reaction between nanoTiB<sub>2</sub> and B<sub>4</sub>C. Iron melts and reacts with B<sub>4</sub>C to form solid ceramic phases (FeB) resulting in porosity reduction and shrinkage associated to liquid phase sintering mechanism.[8]

Typical X-ray diffraction patterns of N5 code from N-Series samples before and after sintering at 2300 °C for 1 hr are shown in Figure 3. Identical to previous analysis, the green sample of N5 code just contains B<sub>4</sub>C and TiB<sub>2</sub> phases similarly (Fig. 3-a). After the heat treatment of the green sample, the diffraction peaks associated with four phases, namely B<sub>4</sub>C, TiB<sub>2</sub>, Ni<sub>3</sub>B and C (Fig. 3-b). It is obvious from Figure 3 that Ni<sub>3</sub>B and C are newly formed phases, and result from the reaction of B<sub>4</sub>C and Ni. The reaction is as follow:



The reaction between Ni and B<sub>4</sub>C leads to release of carbon (Graphite) and formation of the

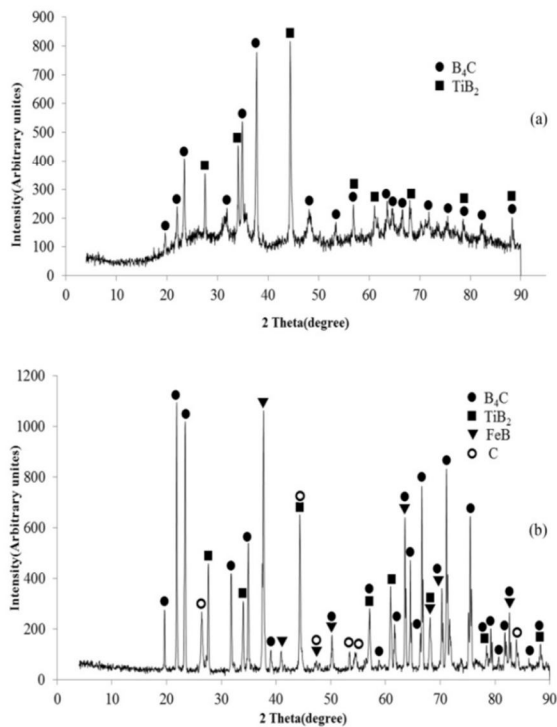
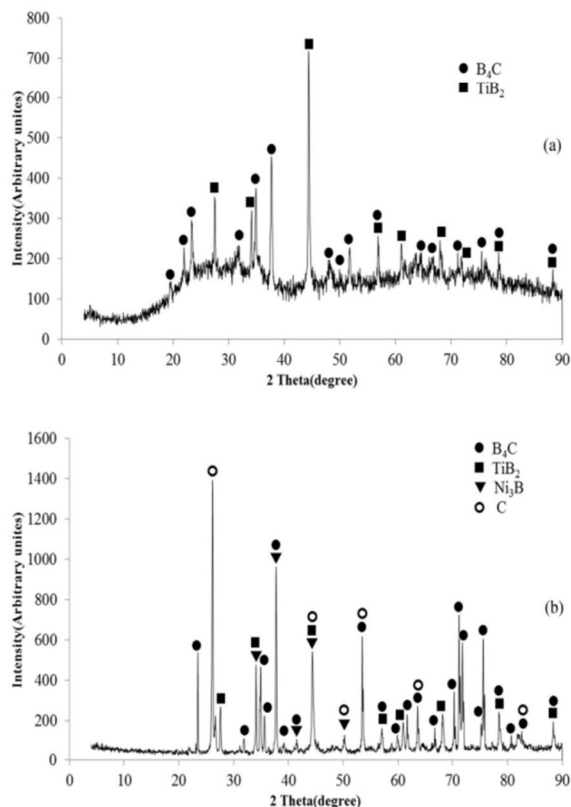


Fig. 1. X-ray diffraction analysis of F6 sample before (a) and after (b) sintering at 2175°C.



**Table 3.** Diffracted planes, 2 theta and d values of graphite.

2Theta (Degree)	d	Diffracted plane
26.42	3.37	002
44.60	2.03	101
63.21	1.16	112



**Fig. 3.** X-ray diffraction analysis of N5 sample before (a) and after (b) sintering at 2175°C.

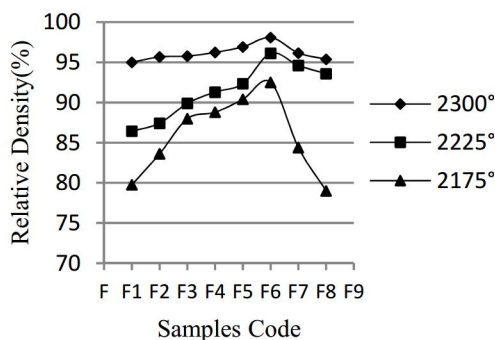


**Fig. 4.** Effect of Fe addition on relative density of F-Series samples sintered at various temperatures.

$Ni_3B$  phase. The relatively low melting point of  $Ni_3B$  (1155 °C) provides the conditions for liquid phase sintering of boron carbide. Diffracted planes, 2 theta and d values of graphite in Figures 1 and 3 are given in table 3.

### 3. 2. Physical and Mechanical Properties

#### 3. 2. 1. Density

Figure 4 shows the effect of Fe addition on relative density of F-Series samples sintered at 2300, 2225 and 2175 °C. It is clear that Fe addition results in an obvious increase of density of nanocomposite. In this Figure one can observe that sample F6 with 3 wt% of Fe has the maximum value of relative density for all of the temperatures. At 2300 °C, more than 98% of theoretical density is obtained for F6 sample. Decreasing of Fe and carbon contents in F7 and F8 samples results in decrease of relative density. Relative density of all samples, sintered at 2300 °C is above 95 % of theoretical density.

The same as Figure 4, Figure 5 shows the effect of Ni addition on relative density of N-Series samples sintered at 2300, 2225 and 2175 °C too. It is shown that Ni addition results in an increase of density of nanocomposite similarly. In this Figure sample N5 with 3 wt% of Ni has the maximum value of relative density for all of the temperatures. At 2300 °C, more than 99% of theoretical density is obtained for N5 sample. Decreasing of Ni and carbon contents in N6 and N7 samples results in decrease of relative density. Relative density of all samples, sintered at 2300 °C is above 97 % of theoretical density.

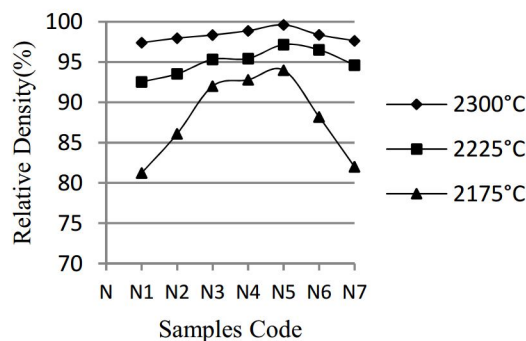


**Fig. 5.** Effect of Ni addition on relative density of N-Series samples sintered at various temperatures.

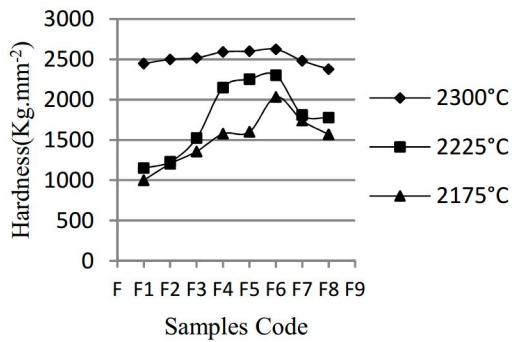


Fig. 6. Effect of Fe addition on hardness of F-Series samples sintered at various temperatures.

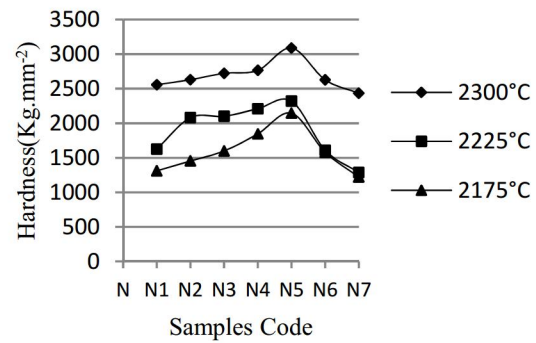


Fig. 7. Effect of Ni addition on hardness of N-Series samples sintered at various temperatures.

From Figure 4 and Figure 5 it can be concluded that addition of both Fe and Ni results in increase of relative density, but the role of Ni addition is more illustrious. By addition of 3 wt% Ni, 99% of theoretical density can be obtained.

### 3. 2. 2. Hardness

Similarly to density, Fe and Ni addition have a positive effect on hardness. Figure 6 shows the effect of Fe additions on hardness of F-Series samples sintered at 2300, 2225 and 2175 °C. As expected, the addition of Fe has a positive effect on Vickers hardness that consists of almost 3wt% Fe loads. This effect can be accounted for the density increase previously pointed out. Hardness increases with Fe content, especially for composites sintered at 2300 °C. F6 sample with 3wt% Fe sintered at this temperature reaches the maximum value of hardness (2624 Kg.mm<sup>-2</sup>). The procedure of hardness variation for samples sintered at various temperatures is shown in this Figure. Decreasing of Fe and carbon contents in F7 and F8 samples results in decrease of hardness.

Figure 7 shows the effect of Ni addition on hardness of N-Series samples sintered at 2300, 2225 and 2175 °C. Similarly to previous part, the addition of Ni has a positive effect on Vickers hardness. In this Figure sample N5 with 3 wt% of Ni has the maximum value of hardness for all of the temperatures. At 2300 °C, the maximum value of hardness (3089.4 Kg.mm<sup>-2</sup>) is obtained for N5 sample.

By comparison between Figure 6 and Figure 7, it can be understood that, the role of Ni addition on improvement of hardness is more illustrious than Fe addition. Almost, all of the N-Series samples sintered at 2300°C have the hardness greater than 2500 Kg.mm<sup>-2</sup>, although some of the F-Series samples sintered at 2300 °C have the hardness greater than 2500 Kg.mm<sup>-2</sup>.

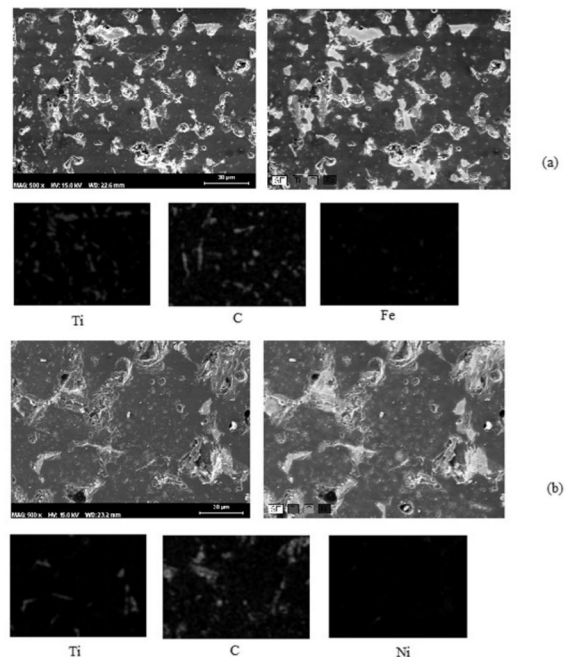


Fig. 8. Map data analysis of F6 sample (a) and N5 sample (b).



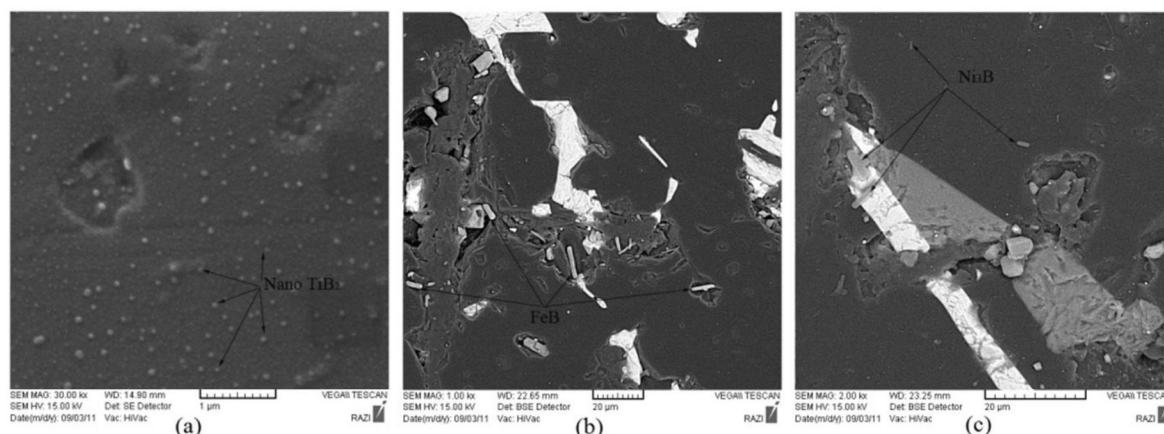


Fig. 9. SEM micrograph analysis of F6 sample for NanoTiB<sub>2</sub> detecting (a), FeB formation (b) and Ni<sub>3</sub>B formation(c).

### 3. 3. Microstructural Analysis

Figure 8 shows the map analysis for both F6 and N5 samples. In this Figure uniform distribution of Ti, Fe, Ni and C is obvious. Figure 9-a shows nano particles of TiB<sub>2</sub> in F6 sample. Size of these particles is about 50 nm. This micrograph confirms the nanocomposite microstructure. Figure 9-b shows the formation of FeB phase in F6 sample and Figure 9-c illustrates the formation of Ni<sub>3</sub>B phase in N5 sample. These SEM micrographs confirm the previous XRD analysis.

### 4. CONCLUSION

In B<sub>4</sub>C-nanoTiB<sub>2</sub> with Fe and Ni addition system, Fe and Ni reacts with B<sub>4</sub>C then FeB, Ni<sub>3</sub>B and free carbon phases are formed. In this system there is not any reaction between TiB<sub>2</sub> and B<sub>4</sub>C. Adding Fe and Ni up to 3wt% to B<sub>4</sub>C-nanoTiB<sub>2</sub> nanocomposites results in increasing the relative density and hardness. But the role of Ni addition on improvement of this physical and mechanical properties is more illustrious than Fe addition. The SEM micrographs confirm the presence of NanoTiB<sub>2</sub> particles and also, FeB and Ni<sub>3</sub>B phases formation.

### ACKNOWLEDGMENTS

The financial support of this work by the

Iranian Nanotechnology Initiative is gratefully acknowledged.

### REFERENCES

1. Dong, H., Zhu, X., Lu, K., "Morphology and composition of nickel–boron nanolayer coating on boron carbide particles", *J. Mater. Sci*, 43, 4247, 2008.
2. Speyer, R. F., Lee, H., "Advances in pressureless densification of boron carbide", *J. Mater. Sci.*, 39, 6017, 2004.
3. Baharvandi, H. R., Hadian, A. M., "Pressureless Sintering of TiB<sub>2</sub>-B<sub>4</sub>C Ceramic Matrix Composite", *J. Mater. Eng. Perf*, 17, 838, 2008.
4. Baharvandi, H. R., Hadian, A. M., Alizadeh, A., "Processing and Mechanical Properties of Boron Carbide–Titanium Diboride Ceramic Matrix Composites", *Appl. Compos. Mater*, 13, 191, 2006.
5. Mashhadi, M., Taheri-Nassaj, E., Sglavo, V. M., "Pressureless sintering of boron carbide", *Ceram. Inter.*, 36, 151, 2010.
6. Baharvandi, H. R., Hadian, A. M., Abdizadeh, H., Ehsani, N., "Investigation on addition of Talc on sintering behavior and mechanical properties of B<sub>4</sub>C", *J. Mater. Eng. Perf*, 15, 280, 2006.
7. Sinaei Pour Fard, H., Baharvandi, H. R., Abdizadeh, H., Shahbahrami, B., "Chemical synthesis of nano-titanium diboride powders by

- borothermic reduction”, *Inter. J. Modern. Physic. B*, 22, 3179, 2008.
8. Mizrahi, I., Raviv, A., Dilman, H., Aizenshtein, M., Dariel, M. P., Frage, N., “The effect of Fe addition on processing and mechanical properties of reaction infiltrated boron carbide-based composites”, *J. Mater. Sci.*, 42, 6923, 2007.
  9. Taherzadeh Mousavian, R., Sharifi, S., Shariat, M. H., “Preparation of nano-structural  $\text{Al}_2\text{O}_3$ - $\text{TiB}_2$  in-situ composite using mechanically activated combustion synthesis followed by intensive milling”, *IJMSE*, 8, 2, 2011.
  10. Hadian Fard, M. J., “Effects of elevated temperature on mechanical behavior of an Aluminium metal matrix composite”, *IJMSE*, 1, 1, 2004.